

Towards Understanding Deep Learning Model in Image Recognition via Coverage Test

Wenkai Li

Hainan University

Haikou, China

cswkli@hainanu.edu.cn

Yingjie Mao

Hainan University

Haikou, China

yingjiemao@hainanu.edu.cn

Xiaoqi Li

Hainan University

Haikou, China

csxqli@ieee.org

Yishun Wang

Hainan University

Haikou, China

yishunwang@hainanu.edu.cn

ABSTRACT

Deep neural networks (DNNs) play a crucial role in the field of artificial intelligence, and their security-related testing has been a prominent research focus. By inputting test cases, the behavior of models is examined for anomalies, and coverage metrics are utilized to determine the extent of neurons covered by these test cases. With the widespread application and advancement of DNNs, different types of neural behaviors have garnered attention, leading to the emergence of various coverage metrics for neural networks. However, there is currently a lack of empirical research on these coverage metrics, specifically in analyzing the relationships and patterns between model depth, configuration information, and neural network coverage. This paper aims to investigate the relationships and patterns of four coverage metrics: primary functionality, boundary, hierarchy, and structural coverage. A series of empirical experiments were conducted, selecting LeNet, VGG, and ResNet as different DNN architectures, along with 10 models of varying depths ranging from 5 to 54 layers, to compare and study the relationships between different depths, configuration information, and various neural network coverage metrics. Additionally, an investigation was carried out on the relationships between modified decision/condition coverage and dataset size. Finally, three potential future directions are proposed to further contribute to the security testing of DNN Models.

CCS CONCEPTS

• Security and privacy → Software security engineering.

KEYWORDS

DNN, Security Testing, Coverage Metrics, Comparison Study, Dataset Size, Model Depths

Permission to make digital or hard copies of all or part of this work for personal or classroom use is granted without fee provided that copies are not made or distributed for profit or commercial advantage and that copies bear this notice and the full citation on the first page. Copyrights for components of this work owned by others than the author(s) must be honored. Abstracting with credit is permitted. To copy otherwise, or republish, to post on servers or to redistribute to lists, requires prior specific permission and/or a fee. Request permissions from permissions@acm.org.

Conference'17, July 2017, Washington, DC, USA

© 2024 Copyright held by the owner/author(s). Publication rights licensed to ACM.

ACM ISBN 978-1-4503-XXXX-X/18/06

<https://doi.org/XXXXXXX.XXXXXXX>

ACM Reference Format:

Wenkai Li, Xiaoqi Li, Yingjie Mao, and Yishun Wang. 2024. Towards Understanding Deep Learning Model in Image Recognition via Coverage Test. In *Proceedings of ACM Conference (Conference'17)*. ACM, New York, NY, USA, 10 pages. <https://doi.org/XXXXXXX.XXXXXXX>

1 INTRODUCTION

Deep Neural Networks (DNNs) play a significant role in the development of deep learning technologies and have been applied to a wide array of specific tasks, including image segmentation, object detection, and pose estimation [22]. A DNN is composed of multiple layers, including input, output, and hidden layers. Compared to shallow neural networks, DNNs construct higher-level features of data by increasing the number of layers. They learn the feature representation of input data in the hidden space by updating the weight information in the neurons through forward or backward propagation. With large-scale AI models being applied to various security-related downstream tasks, such as autonomous vehicle systems and malicious software detection systems [22], DNNs are often used as specific basic functional components [65].

Due to their complex network structure, DNNs may produce different judgments for inputs with minor differences, leading to erroneous results [16, 56, 58]. Therefore, testing DNNs to improve system quality has become extremely important. Existing work uses traditional software testing methods to generate test cases to check for potential vulnerabilities [35]. To evaluate the effectiveness of these generated test cases, various coverage metrics have been proposed, such as neuron coverage [35] and Modified Condition/Decision Coverage (MC/DC) [52]. Also, to focus on the behavior of neurons in different locations within the network structure, various coverage metrics have different characteristics [63]. For example, as shown in Figure 1, statement coverage mainly checks the executable statements involved in the test cases; neuron coverage evaluates the proportion of neurons covered by the test cases.

Many works have focused on the priority of testing inputs [48] to guide security personnel to achieve detection effects in a shorter time, thereby saving resource consumption during testing [6, 13]. Therefore, current empirical research focuses on comparing test case priority indicators [48] with gradient-based attack methods [17] for effectiveness. These methods aim to select more suitable evaluation metrics to generate test cases to evaluate model quality

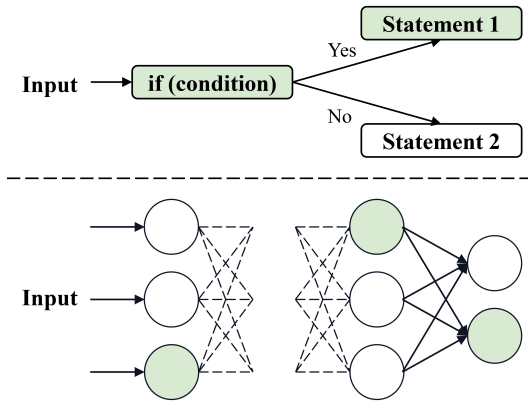


Figure 1: Comparison of traditional code and deep neural network program flow. Above the dotted line is the traditional code flow diagram; below the dotted line is the deep neural network execution diagram. Green indicates the base cell covered by the input example.

[1]. However, these studies on neuron coverage only focus on test cases and lack research that considers the DNN model itself as an influencing factor [47, 55, 61, 70]. Nowadays, many excellent DNN structures have been proposed, such as LeNet, AlexNet, and VGG [22]. DNNs with different structures not only have different model structures but also different model depths. As a model component in AI models, the variation of DNNs is an important factor to be considered [42].

Therefore, to explore the relationship between model depth and various coverage metrics, this paper conducts an empirical study, treating various deep neural networks as black boxes, and testing their relationship with multiple white box coverage metrics. By controlling four variables - the dataset, model structure, model depth, and coverage configuration parameters - through quantitative analysis methods, we analyze the impact of depth changes in deep neural networks of different structures on coverage metrics. In this series of experiments, we selected three different structures of deep neural networks, namely LeNet, VGG, and ResNet, and constructed 10 different deep neural networks ranging from 5 to 54 layers within them. Subsequently, by training each model in the MNIST and CIFAR10 datasets, and using the test set as test case inputs to the model, we analyze each coverage metric.

Contributions. The main contributions are as follows:

- We selected 10 different depth models in the LeNet, VGG, and ResNet neural network structures, respectively, and summarized the rules of their neural network coverage.
- We studied the neuron coverage metrics at different levels to empirically analyze the rules of various coverage metrics under various configuration parameter conditions.
- We conducted LeNet network experiments based on MNIST to analyze the rules of the traditional coverage metric MD/DC, as well as its relationship with neuron coverage.

2 BACKGROUND

In this section, we mainly introduce the coverage metrics of related deep neural networks, including neural network coverage and traditional coverage metrics.

2.1 Neuron Network Coverage

In order to make structured coverage metrics more suitable for deep neural networks, a variety of neural network coverage metrics have been proposed to guide deep neural networks [15, 19, 41, 66]. The operation of software depends on the execution continuity. For example, traditional software depends on the previous statement, while deep neural networks depend on the previous layer of neurons [12, 46, 59, 62]. As shown in Figure 1, the traditional program has branches. After the program runs, the test case input can determine whether there is a problem in the code corresponding to the program statement [4, 14, 40, 57]. Therefore, the more code statements the traditional program covers, the higher the probability of finding code problems. For deep neural networks, the coverage should be based on the neuron activity to determine whether the input has passed through all possible cases [3, 20, 36, 54].

According to the strength of neuronal activity, neural network coverage can be divided into main functional area coverage and boundary area coverage [5, 11, 39]. Moreover, due to the different granularity features in different layers of deep neural networks [29], the layer coverage index is also introduced in this paper.

2.2 Main Functional Area Coverage Indicators

Neuron Coverage. Neuron Coverage (NC) [45] refers to the ratio of the number of neurons whose activation values exceed a threshold when the neural network is input with a test input set to the total number of all neurons [2, 37, 50]. The formula for NC can be expressed as $NCov = \frac{|\{n| \forall i \in T, O(n,i) > t\}|}{|N|}$, where n represents a neuron, and all neurons constitute the set N ; i represents the test input, and all test inputs constitute the set T ; $O()$ represents the activation value of a neuron, $O(n, i)$ means the activation result after inputting i on neuron n ; t is the threshold for a neuron to be activated.

K-multisection Neuron Coverage. K-multisection Neuron Coverage (KMNC) [35] refers to dividing the activation value domain of all neurons into k equal parts, and the ratio of the part covered by the test input set $T = \{x_1, x_2, \dots\}$ to the total part when inputting the neural network [32, 44, 68, 71]. The activation value domain is obtained by inputting the training dataset into the model and observing the activation data statistics of all neurons during the training process. The formula for KMNC can be expressed as $\frac{\sum |\{S_j^n | \exists x \in T; C(x, n) \in S_j^n\}|}{k * |N|}$, where $C(x, n)$ represents the activation value of input instance x in neuron n ; j is a value from 1 to k ; $\frac{|\{S_j^n | \exists x \in T; C(x, n) \in S_j^n\}|}{k}$ represents the KMNC of neuron n .

Neuron Boundary Coverage. The KMNC metric is applied to the activation value range $[L, H]$, i.e., it can only cover $C(x, n)$ in the activation value range [7, 69]. Therefore, the Neuron Boundary Coverage (NBC) metric [35] is defined as the ratio of the number of neurons covered outside the activation value range $(-\infty, L) \cup (H, +\infty)$ to the total number of neurons. The formula for the NBC metric can be represented as $\frac{|\{n | \exists x \in T; C(x, n) \in (-\infty, L) \cup (H, +\infty)\}|}{2 * |N|}$,

where n is a neuron in N [48], and the number of neurons that exist in the lower domain $(-\infty, L)$ and the upper domain $(H, +\infty)$ are both $|N|$. In detail, we denote the size of each region as $\tau = (H-L)/k$. **Strong Neuron Activation Coverage.** Consistent with NBC, Strong Neuron Activation Coverage (SNAC) [35, 67] is also used to detect neuron coverage outside the activation value range. However, to analyze the behavior of highly active neurons in the model, SNAC only considers neurons with activation values in the upper domain, that is, the neuron activation value is within $(H, +\infty)$. In addition, its formula with T as the input case set can be represented as $\frac{|\{n| \exists x \in T; C(x, n) \in (H, +\infty)\}|}{|N|}$.

2.3 Layer Coverage Indicator

Top-k Neuron Coverage. Neuron coverage calculates the proportion of the number of neurons covered by test cases to the total number of neurons [48], while the layer coverage metric calculates the coverage rate from the layer granularity. Top-k Neuron Coverage (TopkNC) [35, 67] refers to the number of times the neurons with the highest activation scores belong to the top k in their layer, that is, the number of the top k neurons on each layer as a proportion of the total number of neurons. The formula for the TopkNC metric can be expressed as $\frac{|\sum_{x \in T} (\sum_{i=1}^l \text{topk}(x, i))|}{|N|}$, where l represents the number of all layers; $\text{topk}(x, i)$ represents the top k neurons with the highest activation scores in the i th layer when x is the input test case.

2.4 Traditional Coverage Indicator

Modified Condition/Decision Coverage. Modified Condition / Decision Coverage (MC/DC) [51] requires both condition and decision coverage, and each decision condition can be influenced by any condition. The core idea is that, for each compound condition, the atomic conditions within it contribute to some positive or negative result of the compound condition, i.e., when the atomic condition changes, the result of the compound condition also changes correspondingly. Consequently, in deep neural networks [53], if a neuron σ at layer l is taken as a decision, then the conditions refer to all neurons at layer $l-1$ that can influence the behavior of neuron σ .

3 EXPERIMENTS

In this section, we mainly introduce the main experimental procedure. First, three key questions related to neuron coverage are posed. We then conducted a series of experiments to answer the following questions.

- RQ 1: How do model depths impact the network coverage?
- RQ 2: How do the parameters impact the network coverage?
- RQ 3: Are traditional coverage metrics effective in networks?

3.1 Experimental Setup

In this paper, we perform experiments on deep neural networks with three different network structures, and there are a total of 10 different numbers of layers. We select LeNet[23] to represent small-scale deep models, and VGG[49] and ResNet[18] to represent large-scale deep models. In addition, VGG uses a sequential structure, while ResNet uses a non-sequential structure. We evaluate the LeNet network structure using the MNIST dataset, and evaluate

the VGG and ResNet network structures using the CIFAR10 dataset. According to the description in Table 1, the MNIST dataset consists of 28x28 grayscale images of handwritten digits, with 60,000 images for training and 10,000 images for testing. The CIFAR10 dataset consists of 32x32 color images, with a total of 10 categories, each containing 6,000 images. In our evaluation process, we randomly select 50,000 images from the CIFAR10 dataset for training, and use the remaining part for testing coverage metrics. All experiment results are completed on a Ubuntu Server 22.04 device equipped with an Intel(R) Core(TM) i9-13900k CPU and NVIDIA GeForce RTX 4070 Ti.

Table 1: The Statistical Information of Datasets

Dataset	Pixel Size	Class Size	Training : Testing
MNIST	28 × 28 × 1	10	60K : 10k
CIFAR10	32 × 32 × 1	10	50K : 10k

3.2 The Neuron Coverage

To explore the influence of different model structures and depths on neuron coverage, we selected three deep models with different structures: LeNet, VGG, and ResNet. Among them, LeNet and VGG adopt a sequential deep network structure, while ResNet adopts a non-sequential deep network structure. In this section, we conduct experiments, which cover models with different depths from 5 to 54 layers, and evaluate the coverage of the neuron coverage metrics at different thresholds. For the small-scale deep model LeNet, the difference between different layers is the number of final fully connected layers. For example, LeNet1 is a sequential deep network architecture with five layers, in order: convolutional layer, average pooling layer, convolutional layer, average pooling layer, and fully connected layer; LeNet4 is a 6-layer structure, and according to the sequential network hierarchy, a layer of fully connected gap exists between LeNet1 and LeNet4; While LeNet5 is a 7-layer structure, its sequential network layer level design has more number of fully connected layers, and this increase number is one.

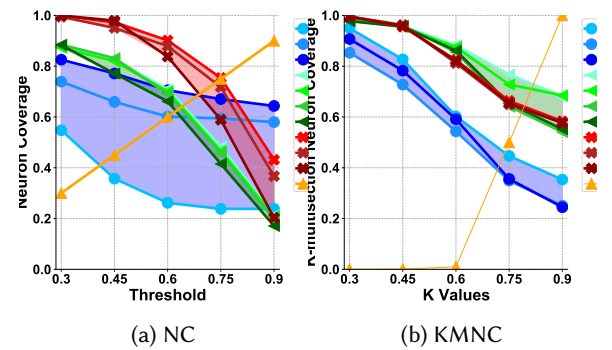


Figure 2: The NC and KMNC in Different Models. Blue groups represent the coverages of LeNets, green groups for VGGs, and red groups for ResNets.

Table 2: Neuron Coverage and K-Multisection Neuron Coverage for Deep Models

Indicators	Parameters	Models									
		LeNet			VGG				ResNet		
		5 layers	6 layers	7 layers	11 layers	13 layers	16 layers	19 layers	21 layers	37 layers	54 layers
NC	$\tau=0.3$	0.5476	0.7391	0.8256	0.8758	0.8728	0.885	0.8833	0.9994	0.9944	0.9995
	$\tau=0.45$	0.3571	0.6594	0.7713	0.8246	0.8196	0.8315	0.7713	0.9726	0.9507	0.9795
	$\tau=0.6$	0.2619	0.6014	0.7054	0.7098	0.7008	0.6908	0.6612	0.9015	0.8789	0.8378
	$\tau=0.75$	0.2381	0.5942	0.6705	0.4823	0.4667	0.4578	0.4152	0.7536	0.7176	0.5888
	$\tau=0.9$	0.2381	0.5797	0.6434	0.2128	0.208	0.196	0.1709	0.4314	0.3671	0.2036
KMNC	$k=10$	0.95	0.8529	0.907	0.983	0.983	0.9811	0.9774	0.9961	0.9958	0.9945
	$k=100$	0.8267	0.7273	0.7824	0.956	0.9542	0.9605	0.9556	0.9555	0.9622	0.9582
	$k=1000$	0.6023	0.5433	0.591	0.8831	0.8753	0.8547	0.8618	0.8246	0.8122	0.8201
	$k=5000$	0.4464	0.3493	0.3559	0.7673	0.7278	0.6414	0.6528	0.6634	0.6502	0.6545
	$k=10000$	0.3536	0.2506	0.2446	0.6814	0.6848	0.5407	0.5521	0.5832	0.5774	0.5765

However, as shown in Figure 2, for the relatively small-scale sequential network structure LeNet, the neuron coverage has an inverse relationship with the threshold, and the rate of neuron coverage decline has an inverse relationship with the number of threshold increases. According to our experimental results, the neuron coverage of the LeNet model structure will tend to a stable value δ as the threshold increases. Specifically, the stable value δ corresponding to LeNet1 is about 0.24, the stable value δ corresponding to LeNet4 is about 0.58, and the stable value δ corresponding to LeNet5 is about 0.64. Moreover, as depth increases, LeNet models with greater depth will have higher neuron coverage. Therefore, compared to the neuron coverage gap between LeNet4 and LeNet5, the gap between LeNet1 and LeNet4 increases with the enhancement of the threshold.

The VGG model consists of a sequential deep network structure composed of five convolutional segments, and different from the way of depth increase of the LeNet model, VGG achieves different depths by adding convolutional layers in different convolutional segments. In this experiment, we tested these deep neural network architectures VGG11 (11 layers), VGG13 (13 layers), VGG16 (16 layers), and VGG19 (19 layers), where the number of layers refers to the number of convolutional and fully connected layers. As shown in Figure 2, at lower thresholds, the neuron coverage metric is difficult to distinguish VGG models with different depths, and the gap between the neuron coverage metrics is not large in the distribution of the individual thresholds. However, according to the results in Table 2, when the threshold is larger than 0.6, the neuron coverage decreases as the depth of the VGG model increases. In addition, we observe that the rate of decline of the neuron coverage metric increases with the threshold, independent of the depth of the model. Therefore, the decreasing trend of neuron coverage in the VGG model is directly opposite to that in the LeNet model.

The ResNet model consists of a network structure consisting of five convolutional segments. However, unlike the VGG model, ResNet employs residual unit connections and is therefore a non-sequential structure. In Table 2, the number of layers represents the total number of convolutional, pooling, and fully connected layers. We explored the relationship between ResNet neural networks with non-sequential structures, such as ResNet18 (21 layers), ResNet34

(37 layers), and ResNet50 (54 layers), and the neuron coverage index. As shown in Figure 2, the neuron coverage is proportional to the model depth at threshold values above 0.6. At thresholds 0.3 and 0.45, ResNet34 has lower neuron coverage than ResNet18 and ResNet50 networks. In addition, the decline rate law of neuron coverage is basically consistent with the VGG model, which increases with the increase of the threshold. However, compared with the VGG model, the neuron coverage of ResNet decreases more obviously, and the rate of decline increases with the depth.

Answer to RQ1. As the model depth increases, the neuron coverage decreases. In addition, since the rate of decline of neuron coverage is related to the model depth as well as the threshold range, the answers to Question one and two are relevant. When the configuration parameter of this coverage metric, namely the threshold, is greater than or equal to 0.6, the rate of decline of LeNet and ResNet models will accelerate as the depth of the model increases. However, when the threshold is 0.3 or 0.45, the decline rate of LeNet and ResNet models also slows down as the model depth increases. In addition, there is a weak correlation between the rate of descent and the depth of the model for the VGG model.

3.3 The K-Multisection Neuron Coverage

The KMNC aims to focus on the main functional regions involved in the trained model to obtain the average coverage of K neurons in the main functional regions of the test set. For the small-scale LeNet model, as shown in Table 2, the highest neuron coverage of the LeNet model is 0.8256, when the threshold is 0.3 and the depth of the model is 7 layers. However, when $k=10$, the KMNC of the LeNet model is significantly higher than 0.8256. This indicates that in some cases, the main functional region of the model already contains most neurons. In addition, as shown in Figure 2, the mean score k of the main functional region has an inverse relationship with the coverage of k -multisection neurons. When the model depth is 5 layers, the k -multisection neuron coverage is higher than that of LeNet4, and the coverage of the LeNet5 model lies in between. As for the answer to question 1, when the model is LeNet, the coverage of k -multisection neurons also decreases with the increase of the model depth, and the rate of decline also increases. When the model is VGG, Figure 6 shows that the k -multisection neuron coverage decreases as the mean score k increases. In addition, the

coverage varies less when increasing the depth of the VGG model from 16 to 19 layers. In addition, further observation reveals that when we do not consider the VGG19 model and the value of k ranges from 100 to 5000, the rate of decline of k -multisection neuron coverage increases with the depth of the model. In addition, there is little difference between the k -multisection neuron coverage of all ResNet neural networks. This indicates that when the deep neural network model is deeper than 19 layers and applied to the CIFAR10 dataset, increasing the model depth does not improve the coverage of neurons in the main functional regions.

Answer to RQ2. The coverage of KMNC for all deep models decreases as the configuration parameter, the segmentation value k , increases. In addition, when the value of $k \in (10,5000)$, this coverage drop rate increases, and the subsequent drop rate decreases.

3.4 Neuron Boundary Coverage

Boundary region coverage metrics include neuron boundary coverage and strong neuron activation coverage. The neuron boundary coverage metric focuses on how active a neuron is in extreme states, namely edge activity. We use the activity difference to divide the main functional area and the boundary area. Therefore, in order to investigate the relationship between neuronal activity outside the main functional area and different configuration parameters, we mainly analyzed neuronal boundary coverage and strong neuronal activation coverage.

According to the results in Table 3, we conducted experiments with different depths of LeNet models under different configuration parameters. Here, ε represents the distance from the boundary of the main functional area, and τ represents the size of a single partitioned region in the coverage of k -multiregion neurons. In other words, in the experiment, the neurons boundary scope of coverage concern for $(-\infty, L - \varepsilon) \cup (H + \varepsilon, +\infty)$, and strong neuron activation coverage scope of attention $(H + \varepsilon, +\infty)$. In addition, in order to quantitatively analyze the impact of model depth as well as boundary distance on coverage, the experiment in Table 3 fixed the number of divided regions to 1000. Figure 8 shows that this coverage has different laws for boundary distances $\varepsilon < 0$ and $\varepsilon > 0$.

Answer to RQ1. At boundary distance $\varepsilon < 0$, the rate of decrease of the neuron boundary coverage is proportional to the depth of the model. However, when $\varepsilon > 0$ and increases infinitely, when the range of the boundary region shrinks, this value has a weak relationship with the model depth and is stable around a certain value.

Answer to RQ2. The neuron boundary coverage is high at the boundary distance $\varepsilon < 0$ and decreases as the absolute value of the boundary distance shrinks. This also indirectly reflects the effectiveness of coverage detection of neurons in the main functional area. However, when $\varepsilon > 0$, the coverage of the neurons at the edge of the model gradually decreases and tends to 0. It is worth noting that the neuron boundary coverage in this range has a similar rate of decline.

3.5 Strong Neuron Activation Coverage

As shown in Figure 3, the model depth has an inverse relationship with the initial value of strong neuron activation coverage, and this coverage decreases as the boundary distance increases. When the boundary distance $\varepsilon < 0$, that is, for the neurons whose activation

Table 3: Neuron Boundary Coverage and Strong Neuron Activation Coverage for Deep Models

Indicators	Parameters	LeNet		
		5 layers	6 layers	7 layers
NBC	$\varepsilon = -1.5 * \tau$	0.0714	0.082	0.0886
	$\varepsilon = -1 * \tau$	0.066	0.0794	0.0886
	$\varepsilon = -0.5 * \tau$	0.0411	0.0471	0.0486
	$\varepsilon = 0 * \tau$	0.0087	0.0066	0.006
	$\varepsilon = 0.5 * \tau$	0.0043	0.0059	0.0056
	$\varepsilon = 1 * \tau$	0.0043	0.0059	0.0056
	$\varepsilon = 1.5 * \tau$	0.0043	0.0053	0.0056
	$\varepsilon = 2 * \tau$	0.0043	0.0049	0.0056
	$\varepsilon = -1.5 * \tau$	0.2738	0.1812	0.1182
SNAC	$\varepsilon = -1 * \tau$	0.2024	0.1667	0.1182
	$\varepsilon = -0.5 * \tau$	0.1548	0.1449	0.1008
	$\varepsilon = 0 * \tau$	0.0357	0.0543	0.062
	$\varepsilon = 0.5 * \tau$	0.0238	0.0543	0.00581
	$\varepsilon = 1 * \tau$	0.0238	0.0543	0.0581
	$\varepsilon = 1.5 * \tau$	0.0238	0.0507	0.0581
	$\varepsilon = 2 * \tau$	0.0238	0.0507	0.0581

range is near the boundary H of the upper domain, the decline rate of the activation coverage of strong neurons slows down with the increase of the depth of the model. Therefore, the neurons with higher activity in the main functional area are more widely distributed in the shallow model. However, when the boundary distance $\varepsilon > 0$, the rate of decrease of strong neuron activation coverage approaches 0.

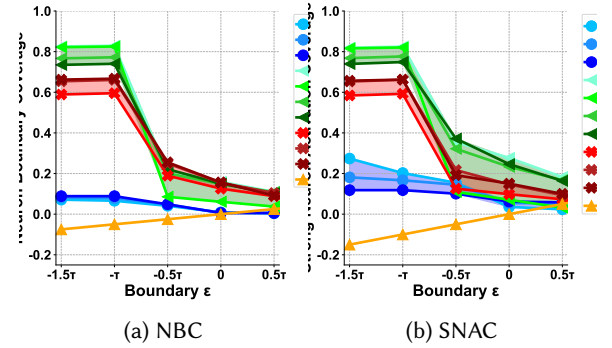


Figure 3: The NBC and SNAC in Different Models. Blue groups represent the coverages of LeNets, green groups for VGGs, and red groups for ResNets.

In particular, to quantitatively analyze the neuron boundary coverage of the VGG and ResNet models trained on the CIFAR10 dataset, we fixed the partition region τ to 10000.

Since the neuron boundary coverage index focuses on neurons in two regions of the upper and lower boundary, that is, hyperactive and inactive neurons, we jointly analyze the two coverage indices in Table 3 in order to accurately understand the activity rules of strong and weak activity neurons.

Table 4: Top-K Neuron Coverage for Deep Models

Indicator	Parameters	Model									
		LeNet			VGG				ResNet		
		5 layers	6 layers	7 layers	11 layers	13 layers	16 layers	19 layers	21 layers	37 layers	54 layers
Top-K NC	k=5	0.9619	0.8304	0.8062	0.1933	0.1923	0.1717	0.1612	0.4004	0.3387	0.1619
	k=10	0.8857	0.8159	0.824	0.2657	0.2701	0.2554	0.2384	0.5499	0.4687	0.2359
	k=15	0.6667	0.7667	0.823	0.3158	0.3169	0.3155	0.2938	0.6509	0.5698	0.2924
	k=20	0.5	0.7163	0.8047	0.352	0.352	0.3615	0.3404	0.7214	0.653	0.3383
	k=25	0.4	0.6858	0.7957	0.3834	0.3814	0.393	0.3792	0.7865	0.724	0.3802
	k=30	0.3333	0.6659	0.7903	0.4084	0.4059	0.4223	0.4108	0.8339	0.7878	0.4181
	k=35	0.2857	0.6482	0.787	0.4308	0.4297	0.4483	0.4356	0.8748	0.8338	0.4501

When the boundary distance $\varepsilon \in (0, 0.2\tau)$, the values of neuron boundary coverage and strong neuron activation coverage, and their change rates are different in different models. For the VGG model, the value of strong neuron activation coverage is higher than that of neuron boundary coverage, and its decline rate is also positively correlated with the coverage value. This indicates that as the boundary region expands, the number of neurons in the upper boundary decreases. The number of strongly active neurons gradually decreases. Moreover, the number of neurons in the upper boundary is higher than the sum of the number of neurons in the lower and upper boundaries. Thus, within the boundary distance $\varepsilon \in (0, 0.2\tau)$, weakly active neurons are negative in the model.

However, when the boundary distance $\varepsilon < 0$, the distribution rules of the neuron boundary coverage and strong neuron activation coverage of the VGG and ResNet models are similar, while there are some slight differences when the boundary distance $\varepsilon > 0$. When the boundary distance $\varepsilon > 0.2\tau$, the VGG model coverage and its change rate tend to be stable from 13 to 19 layers. It is worth noting that when the VGG11 model is within the boundary distance $\varepsilon \in (0.4\tau, 0.5\tau)$, its neuron boundary coverage increases, while the strong neuron activation rate decreases. This means that the number of weakly active neurons in this range increases without affecting the performance of the model.

In the range of boundary distance $\varepsilon \in (-0.1\tau, 0)$ for VGG and ResNet model structures, the decline rate of neuron boundary coverage is high, and it shows a sharp decline trend near $\varepsilon=0$. This phenomenon indicates that the model is close to fit at $\varepsilon=0$, while the neuron activation values vary greatly from -0.1τ to 0 region, which indicates that this coverage index can be effectively localized to the boundary.

Answer to RQ1. In the LeNet model, the reaching value of the strong neuron activation coverage is proportional to the model depth. When the number of model layers is similar, the difference in the reaching value of strong neuron activation coverage decreases with the increase of depth. Assuming $\phi(\alpha, \beta)$ model the coverage of strong neuron activation of α and β are absolute value, the $\phi(L(5), L(6)) - \phi(L(6), L(7)) > 0$. Here, $L(\gamma)$ denotes the LeNet model with γ layers. Moreover, in the range of boundary distance $\varepsilon \in (-0.1\tau, 0)$, the VGG model has the highest rate of decline at depth 13, and the rate of decline is negatively correlated with depth at other depths. However, the neuron boundary coverage of the ResNet model is positively correlated with depth,

and the difference in neuron boundary coverage between models with a similar number of layers decreases with the increase of depth. Assume, in other words, $\omega(\alpha, \beta)$ means the model of alpha and beta neurons boundary coverage or absolute difference, the $\omega(R(21), R(37)) - \omega(R(37), R(54)) > 0$. The $R(\gamma)$ represents the ResNet model with γ layers.

Answer to RQ2. In the LeNet model, the activation coverage of strong neurons decreases with the increase of the threshold boundary distance ε . In addition, its decline rate also increases with the increase of ε , and this coverage and its decline rate stabilize around a fixed value at $\varepsilon=0$.

3.6 Top-k Neuron Coverage

Since the three models with different depths of the LeNet structure are trained based on the MNIST dataset, the training and testing process of models such as VGG and ResNet are performed on the CIFAR10 dataset. Therefore, we analyze the coverage of Top-k neurons for LeNet as well as for VGG and ResNet neural network architectures, respectively. Based on the data in Table 5, we summarize multiple Top-k neuron coverage test results in the range of threshold k from 5 to 35.

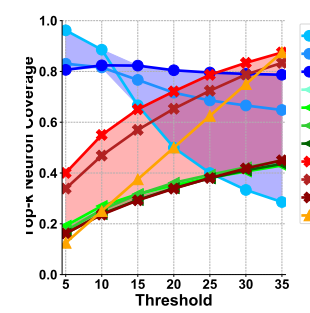


Figure 4: The TopKNC in Different Models. Blue groups represent the coverages of LeNets, green groups for VGGs, and red groups for ResNets.

Answer to RQ1. For the LeNet model, the rate of Top-k neuron coverage change is negatively correlated with the model depth. Moreover, for the LeNet model with a similar number of layers, the difference in Top-k neuron coverage between them decreases as the depth increases. Assuming $\mu(\alpha, \beta)$ model of alpha and beta Top - k

Table 5: Modified Condition/Decision Coverage for Deep Models

Model	Indicator	Dataset Size						
		100	200	400	800	1600	3200	6400
LeNet (5 layers)	MC/DC(SS)	0.0192	0.0337	0.0385	0.0481	0.0481	0.0529	0.0577
	MC/DC(SV)	0.2115	0.3702	0.3846	0.4904	0.5	0.5769	0.6346
	MC/DC(VS)	0.0769	0.1346	0.1538	0.1923	0.1923	0.2115	0.2308
	MC/DC(VV)	1	1	1	1	1	1	1
LeNet (6 layers)	MC/DC(SS)	0.1443	0.1957	0.2107	0.2823	0.2933	0.306	0.3568
	MC/DC(SV)	0.082	0.1143	0.1467	0.2003	0.2431	0.2621	0.3031
	MC/DC(VS)	0.5404	0.5439	0.5439	0.5577	0.5577	0.5577	0.5681
	MC/DC(VV)	0.6686	0.6715	0.6721	0.6721	0.6721	0.6744	0.6744
LeNet (7 layers)	MC/DC(SS)	0.0186	0.0409	0.051	0.0661	0.0945	0.0969	0.1194
	MC/DC(SV)	0.0125	0.0269	0.0353	0.0454	0.06	0.0692	0.0855
	MC/DC(VS)	0.1304	0.132	0.1335	0.1339	0.1355	0.1572	0.1531
	MC/DC(VV)	0.1489	0.1503	0.1519	0.1528	0.1532	0.1567	0.1568

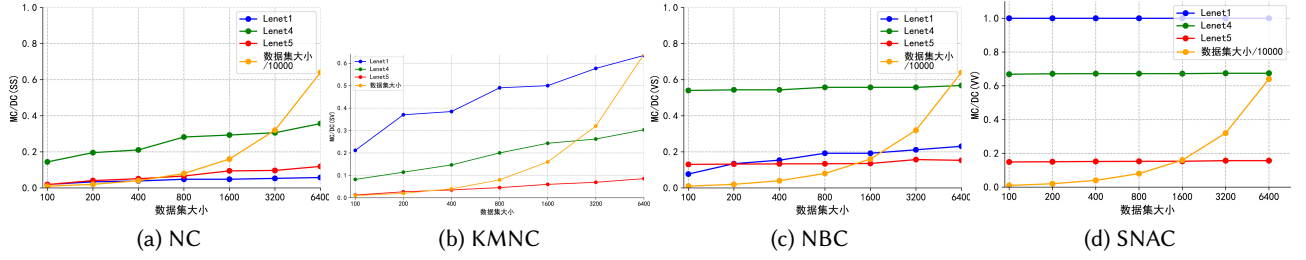


Figure 5: The MC/DC Coverage.

coverage in neurons are absolute value, then we get $\mu(L(5), L(6)) - \mu(L(6), L(7)) > 0$. $L(\gamma)$ represents the LeNet network structure with γ layers. Therefore, there is an important relationship between Top-k neuron coverage and model depth in LeNet, a small-scale sequential deep neural network. Top-k neuron coverage counts the total number of strongly active neurons in each layer. However, the number of layers of the model is positively related to the stability of this coverage. Therefore, compared with LeNet1 and LeNet4, the number of strongly active neurons in each layer in LeNet5 is more evenly distributed. In the VGG model, this coverage is weakly correlated with model depth. For the experimental results of the non-sequential neural network structure ResNet in Figure 16, its Top-k neuron coverage is negatively correlated with the model depth, and the Top-k neuron coverage value is higher than the case of the VGG model as a whole. The absolute value of the difference in Top-k neuron coverage of ResNet models with similar layers decreases with decreasing depth, such as $\mu(L(37), L(54)) > \mu(L(21), L(37))$.

Answer to RQ2. Different deep models of the sequential neural network architecture VGG have similar patterns in the Top-k neuron coverage index. As the threshold k increases, the coverage of Top-k neurons in the VGG model increases, but its change rate gradually decreases. More, as the threshold value increases, the change rate of Top-k neuron coverage gradually slows down and approaches zero.

3.7 Modified Condition/Decision Coverage

The MC/DC test index mainly focuses on all the conditions related to the decision; in other words, for each decision, the conditions in its previous layer that can affect the decision. However, to fully analyze these determinations and conditions, we focus on four different coverage methods: Sign-Sign (SS), Sign-Value (SV), Value-Sign (VS), and Value-Value (VV). Here, the sign and the decision represent the function used to detect the change of the activation value of the neuron when the input value changes. We tested this data on different dataset sizes. Also, all other relevant configuration parameters are the same as those in DeepHunter[64].

Answer to RQ3. We summarize the four covering method regularities shown in Figure 5. In the four coverage methods, even though there are curves with a low change rate, all the coverage rates increase with the increase of the dataset size. Among them, MC/DC(VV) has the highest coverage value and has little relationship with the dataset. In addition, the coverage value is inversely proportional with the model depth, and $\xi(L(5), L(6)) - \xi(L(6), L(7)) > 0$, the $\xi(\alpha, \beta)$ shows two models of α and β MC/DC (VV) the difference between the absolute value. In addition, the MC/DC (SV) is also inversely proportional to the model depth.

In order to clearly answer the difference between MC/DC and other coverage metrics, we make a comparative analysis from the perspective of model depth, configuration parameters, and change rate. For the model depth, the activation coverage of neurons, strong

neurons with boundary distance greater than 0 has a positive correlation law, and the coverage of Top-k neurons, MC/DC (SV), and MC/DC (VV) has a negative correlation law. For the configuration parameters of various indicators, the activation coverage of neurons, Top-k neurons, and strong neurons with boundary distance less than a certain value has a negative correlation law. Strong neuronal activation, MC/DC (SS), MC/DC (SV), MC/DC (VS), and MC/DC (VV) coverage have positive correlation laws for boundary distance greater than 0. In addition, for the rate of change, neurons, strong neuron activation, Top-k neurons, MC/DC (SV), MC/DC (VV) coverage have a negative correlation law with model depth, and neuron boundary coverage has a positive correlation law with model depth.

4 FUTURE WORK

Deep neural network models are widely used in feature extraction for many downstream tasks such as image segmentation, object detection, and pose estimation. With the wide application of deep neural networks, model security testing has also attracted a lot of attention [8, 9, 21, 24–28, 30, 31, 33, 34, 38, 43, 60, 72]. Therefore, in order to test the security of these models, various coverage metrics have been proposed to detect model units covered by input test cases [45, 48, 52]. The influencing factors of the coverage detection effect were explored to improve the evaluation accuracy of the test cases on the model. The main process of the coverage index in the model is improved to enhance the interpretability of the deep neural network. In summary, future research on DNN coverage may have the following directions.

- (1) **Improving the theoretical research system of deep neural network coverage.** At present, the research on neural network coverage index mostly focuses on the design of new neuron coverage index and coverage test priority technology [1, 48]. However, for deep neural networks, there is no unified evaluation index for the neuron behavior involved in the coverage index. Although some existing studies analyze the data flow of test input by studying the topology structure in the network. However, there is a lack of relevant neuron behavior analysis to improve the interpretability of the test model. Therefore, it is of great significance to establish an effective analysis framework for neuron coverage and improve the theoretical research system of deep neural network coverage.
- (2) **Exploring the effective combination of various coverage index detection models.** Due to the different emphasis of various coverage indicators, they have different time resource consumption under different configuration parameters. Recent studies have designed a variety of test case priorities to guide different test cases [10, 45, 48], and improved the testing effectiveness of neural network models by optimizing the input of test cases. However, not only test cases, but also the selection priority of coverage metrics affect the efficiency of testing work. Therefore, the design of the coverage priority method and the empirical analysis of a variety of coverage combination detection models can provide more efficient model testing work, and also help to explore testing strategies from more perspectives.

- (3) **Designing an effective test system for different structural models.** Although the sequential network structure model and the non-sequential network structure model have the same regular relationship with their configuration parameters and model depth when facing the input samples, there are obvious differences in the layer index Top-k neuron coverage. Therefore, it is of great significance to design a universal structural coverage index for different structural models to break through the structural test of deep neural networks with complex structures.

5 CONCLUSION

This paper presents an empirical study of coverage metrics in deep neural networks. First, we illustrate the coverage metric and the traditional coverage metric MC/DC. Then, we point out the relationship between model depth, configuration parameters with respect to different coverage metrics, and the regular relationship at different configuration cases. To answer these questions, we conduct extensive empirical experiments on 6 different coverage rates in 10 deep neural models with different number of layers to investigate the properties of various coverage rates. Finally, we provide the future research directions of coverage metrics in deep neural networks, hoping that we can provide comprehensive cognition and reference for researchers interested in coverage work, and make further contributions to the security testing of DNNs.

REFERENCES

- [1] Zohreh Aghababayan, Manel Abdellatif, Lionel Briand, Mojtaba Bagherzadeh, and et al. Black-box testing of deep neural networks through test case diversity 2023. *IEEE Transactions on Software Engineering* 49, 5, 3182–3204.
- [2] Qurat Ul Ain, Wasi Haider Butt, Muhammad Waseem Anwar, Farooque Azam, and Bilal Maqbool. A systematic review on code clone detection 2019. *IEEE access* 7, 86121–86144.
- [3] Lennart Ante. The non-fungible token (NFT) market and its relationship with Bitcoin and Ethereum 2022. *FinTech* 1, 3, 216–224.
- [4] Lennart Ante. Non-fungible token (NFT) markets on the Ethereum blockchain: Temporal development, cointegration and interrelations 2023. *Economics of Innovation and New Technology* 32, 8, 1216–1234.
- [5] Iz Beltagy, Matthew E Peters, and Arman Cohan. Longformer: The long-document transformer 2020. *arXiv preprint arXiv:2004.05150*.
- [6] Karthikeyan Bhargavan, Antoine Delignat-Lavaud, Cédric Fournet, Anitha Golamudi, Georges Gonthier, Nadim Kobeissi, Natalia Kulatova, Aseem Rastogi, Thomas Sibut-Pinote, Nikhil Swamy, et al. Formal verification of smart contracts: Short paper 2016. In *Proceedings of the 2016 ACM workshop on programming languages and analysis for security*, 91–96.
- [7] Piotr Bojanowski, Edouard Grave, Armand Joulin, and Tomas Mikolov. Enriching word vectors with subword information 2017. *Transactions of the association for computational linguistics* 5, 135–146.
- [8] Jiuyang Bu, Wenkai Li, Zongwei Li, Zeng Zhang, and Xiaoqi Li. Enhancing smart contract vulnerability detection in dapps leveraging fine-tuned llm 2025. *arXiv preprint arXiv:2504.05006*.
- [9] Jiuyang Bu, Wenkai Li, Zongwei Li, Zeng Zhang, and Xiaoqi Li. SmartBugBert: BERT-Enhanced Vulnerability Detection for Smart Contract Bytecode 2025. *arXiv preprint arXiv:2504.05002*.
- [10] Huihi Chen, Cheng Fu, Jishen Zhao, and Farinaz Koushanfar. Deepinspect: A black-box trojan detection and mitigation framework for deep neural networks. 2019. In *Proceedings of the International Joint Conferences on Artificial Intelligence*, Vol. 2, 8.
- [11] Krzysztof Chormanski, Valerii Likhoshesterov, David Dohan, Xingyou Song, Andreea Gane, Tamas Sarlos, Peter Hawkins, Jared Davis, Afroz Mohiuddin, Lukasz Kaiser, et al. Rethinking attention with performers 2020. *arXiv preprint arXiv:2009.14794*.
- [12] Hanting Chu, Pengcheng Zhang, Hai Dong, Yan Xiao, Shunhui Ji, and Wenrui Li. A survey on smart contract vulnerabilities: Data sources, detection and repair 2023. *Information and Software Technology* 159, 107221.
- [13] João F Ferreira, Pedro Cruz, Thomas Durieux, and Rui Abreu. SmartBugs: A Framework to Analyze Solidity Smart Contracts 2020. In *Proceedings of the 35th*

IEEE/ACM International Conference on Automated Software Engineering. 1349–1352.

[14] Zhipeng Gao, Lingxiao Jiang, Xin Xia, David Lo, and John Grundy. Checking Smart Contracts with Structural Code Embedding 2020. *IEEE Transactions on Software Engineering*.

[15] Asem Ghaleb and Karthik Pattabiraman. How effective are smart contract analysis tools? evaluating smart contract static analysis tools using bug injection 2020. In *Proceedings of the 29th ACM SIGSOFT international symposium on software testing and analysis*. 415–427.

[16] Asem Ghaleb, Julia Rubin, and Karthik Pattabiraman. Achecker: Statically detecting smart contract access control vulnerabilities 2023. In *2023 IEEE/ACM 45th International Conference on Software Engineering (ICSE)*. IEEE, 945–956.

[17] Ian J Goodfellow, Jonathon Shlens, and Christian Szegedy. Explaining and harnessing adversarial examples 2014. *arXiv preprint arXiv:1412.6572*.

[18] Kaiming He, Xiangyu Zhang, Shaoqing Ren, and Jian Sun. Deep residual learning for image recognition 2016. In *Proceedings of the IEEE conference on computer vision and pattern recognition (CVPR)*. 770–778.

[19] Ningyu He, Lei Wu, Haoyu Wang, Yao Guo, and Xuxian Jiang. Characterizing code clones in theethereum smart contract ecosystem 2020. In *Financial Cryptography and Data Security: 24th International Conference, FC 2020, Kota Kinabalu, Malaysia, February 10–14, 2020 Revised Selected Papers 24*. Springer, 654–675.

[20] Jianjun Huang, Songming Han, Wei You, Wenchang Shi, Bin Liang, Jingzheng Wu, and Yanjun Wu. Hunting vulnerable smart contracts via graph embedding based bytecode matching 2021. *IEEE Transactions on Information Forensics and Security* 16, 2144–2156.

[21] Dechao Kong, Xiaoqi Li, and Wenkai Li. Characterizing the Solana NFT ecosystem 2024. In *Companion Proceedings of the ACM Web Conference 2024*. 766–769.

[22] Nikolas Kriegeskorte and Tal Golan. Neural network models and deep learning 2019. *Current Biology* 29, 7, R231–R236.

[23] Yann LeCun, Léon Bottou, Yoshua Bengio, and Patrick Haffner. Gradient-based learning applied to document recognition 1998. *Proc. IEEE* 86, 11, 2278–2324.

[24] Wenkai Li, Xiaoqi Li, Zongwei Li, and Yuqing Zhang. Cobra: interaction-aware bytecode-level vulnerability detector for smart contracts 2024. In *Proceedings of the 39th IEEE/ACM International Conference on Automated Software Engineering*. 1358–1369.

[25] Wenkai Li, Zhipie Liu, Xiaoqi Li, and Sen Nie. Detecting Malicious Accounts in Web3 through Transaction Graph 2024. In *Proceedings of the 39th IEEE/ACM International Conference on Automated Software Engineering*. 2482–2483.

[26] Xiaoqi Li et al. Hybrid analysis of smart contracts and malicious behaviors in ethereum 2021.

[27] Xiaoqi Li, Ting Chen, Xiapu Luo, and Chenxu Wang. CLUE: towards discovering locked cryptocurrencies in ethereum 2021. In *Proceedings of the 36th Annual ACM Symposium on Applied Computing*. 1584–1587.

[28] Xiaoqi Li, L Yu, and XP Luo. 2017. On Discovering Vulnerabilities in Android Applications. In *Mobile Security and Privacy*. Elsevier, 155–166.

[29] Yuanchun Li, Ziqi Zhang, Bingyan Liu, Ziyue Yang, and Yunxin Liu. ModelDiff: Testing-based DNN similarity comparison for model reuse detection 2021. In *Proceedings of the 30th ACM SIGSOFT International Symposium on Software Testing and Analysis (ISSTA)*. 139–151.

[30] Zongwei Li, Wenkai Li, Xiaoqi Li, and Yuqing Zhang. StateGuard: Detecting State Derailment Defects in Decentralized Exchange Smart Contract 2024. In *Companion Proceedings of the ACM Web Conference 2024*. 810–813.

[31] Zongwei Li, Xiaoqi Li, Wenkai Li, and Xin Wang. SCALM: Detecting Bad Practices in Smart Contracts Through LLMs 2025. *arXiv preprint arXiv:2502.04347*.

[32] Wei Liang, Yaqin Liu, Ce Yang, Songyou Xie, Kuanching Li, and Willy Susilo. On identity, transaction, and smart contract privacy on permissioned and permissionless blockchain: A comprehensive survey 2024. *Comput. Surveys* 56, 12, 1–35.

[33] Zekai Liu and Xiaoqi Li. SoK: Security Analysis of Blockchain-based Cryptocurrency 2025. *arXiv preprint arXiv:2503.22156*.

[34] Zekai Liu, Xiaoqi Li, Hongli Peng, and Wenkai Li. GasTrace: Detecting Sandwich Attack Malicious Accounts in Ethereum 2024. In *2024 IEEE International Conference on Web Services (ICWS)*. IEEE, 1409–1411.

[35] Lei Ma, Felix Juefei-Xu, Fuyuan Zhang, Jiyuan Sun, Minhui Xue, Bo Li, Chunyang Chen, Ting Su, Li Li, Yang Liu, and et al. Deepgauge: Multi-granularity testing criteria for deep learning systems 2018. In *Proceedings of the 33rd ACM/IEEE international conference on automated software engineering (ASE)*. 120–131.

[36] Wei Ma, Daoyuan Wu, Yuqiang Sun, Tianwen Wang, Shangqing Liu, Jian Zhang, Yue Xue, and Yang Liu. Combining Fine-Tuning and LLM-based Agents for Intuitive Smart Contract Auditing with Justifications 2024. *arXiv preprint arXiv:2403.16073*.

[37] Yu A Malkov and Dmitry A Yashunin. Efficient and robust approximate nearest neighbor search using hierarchical navigable small world graphs 2018. *IEEE transactions on pattern analysis and machine intelligence* 42, 4, 824–836.

[38] Yingjie Mao, Xiaoqi Li, Wenkai Li, Xin Wang, and Lei Xie. SCLA: Automated Smart Contract Summarization via LLMs and Semantic Augmentation 2024. *arXiv preprint arXiv:2402.04863*.

[39] Tomas Mikolov. Efficient estimation of word representations in vector space 2013. *arXiv preprint arXiv:1301.3781*.

[40] Matthieu Nadini, Laura Alessandretti, Flavio Di Giacinto, Mauro Martino, Luca Maria Aiello, and Andrea Baronchelli. Mapping the NFT revolution: market trends, trade networks, and visual features 2021. *Scientific reports* 11, 1, 20902.

[41] Iulian Neamtiu, Jeffrey S Foster, and Michael Hicks. Understanding source code evolution using abstract syntax tree matching 2005. In *Proceedings of the 2005 international workshop on Mining software repositories*. 1–5.

[42] Thao Nguyen, Maithra Raghu, and Simon Kornblith. Do wide and deep networks learn the same things? uncovering how neural network representations vary with width and depth 2020. *arXiv preprint arXiv:2010.15327*.

[43] Yuanzheng Niu, Xiaoqi Li, Hongli Peng, and Wenkai Li. Unveiling wash trading in popular NFT markets 2024. In *Companion Proceedings of the ACM Web Conference 2024*. 730–733.

[44] Michele Pasqua, Andrea Benini, Filippo Contro, Marco Crosara, Mila Dalla Preda, and Mariano Ceccato. Enhancing Ethereum smart-contracts static analysis by computing a precise Control-Flow Graph of Ethereum bytecode 2023. *Journal of Systems and Software* 200, 111653.

[45] Kexin Pei, Yinzhai Cao, Junfeng Yang, and Suman Jana. Deepxplore: Automated whitebox testing of deep learning systems 2017. In *proceedings of the 26th Symposium on Operating Systems Principles (SOSP)*. 1–18.

[46] Peng Qian, Zhenguang Liu, Qinming He, Butian Huang, Duanzheng Tian, and Xun Wang. Smart contract vulnerability detection technique: A survey 2022. *arXiv preprint arXiv:2209.05872*.

[47] Hitesh Sajnani, Vaibhav Saini, Jeffrey Svajlenko, Chanchal K Roy, and Cristina V Lopes. Sourcererc: Scaling code clone detection to big-code 2016. In *Proceedings of the 38th international conference on software engineering*. 1157–1168.

[48] Ying Shi, Beibei Yin, Zheng Zheng, and Tiancheng Li. An empirical study on test case prioritization metrics for deep neural networks 2021. In *Proceedings of the IEEE 21st International Conference on Software Quality, Reliability and Security (QRS)*. 157–166.

[49] Karen Simonyan and Andrew Zisserman. Very deep convolutional networks for large-scale image recognition 2014. *arXiv preprint arXiv:1409.1556*.

[50] Rakshith S Srinivasa, Cao Xiao, Lucas Glass, Justin Romberg, and Jimeng Sun. Fast graph attention networks using effective resistance based graph sparsification 2020. *arXiv preprint arXiv:2006.08796*.

[51] Youcheng Sun, Xiaowei Huang, Daniel Kroening, James Sharp, Matthew Hill, and Rob Ashmore. Testing deep neural networks 2018. *arXiv preprint arXiv:1803.04792*.

[52] Youcheng Sun, Xiaowei Huang, Daniel Kroening, James Sharp, Matthew Hill, and Rob Ashmore. DeepConcolic: Testing and debugging deep neural networks 2019. In *Proceedings of the IEEE/ACM 41st International Conference on Software Engineering (ICSE)*. 111–114.

[53] Youcheng Sun, Xiaowei Huang, Daniel Kroening, James Sharp, Matthew Hill, and Rob Ashmore. Structural test coverage criteria for deep neural networks 2019. *ACM Transactions on Embedded Computing Systems (TECS)* 18, 5s, 1–23.

[54] Nick Szabo. Smart contracts: building blocks for digital markets 1996. *EXTROPY: The Journal of Transhumanist Thought*, 16, 18, 2, 28.

[55] Zhenzhou Tian, Yaqian Huang, Jie Tian, Zhongmin Wang, Yanping Chen, and Lingwei Chen. Ethereum Smart Contract Representation Learning for Robust Bytecode-Level Similarity Detection. 2022. In *SEKE*. 513–518.

[56] Sergei Tikhomirov, Ekaterina Voskresenskaya, Ivan Ivanitskiy, Ramil Takhaviev, Evgeny Marchenko, and Yaroslav Alexandrov. Smartcheck: Static analysis of ethereum smart contracts 2018. In *Proceedings of the 1st international workshop on emerging trends in software engineering for blockchain*. 9–16.

[57] Palina Tolmach, Yi Li, Shang-Wei Lin, Yang Liu, and Zengxiang Li. A survey of smart contract formal specification and verification 2021. *ACM Computing Surveys (CSUR)* 54, 7, 1–38.

[58] Petar Tsankov, Andrei Dan, Dana Drachsler-Cohen, Arthur Gervais, Florian Buerzli, and Martin Vechev. Security: Practical security analysis of smart contracts 2018. In *Proceedings of the 2018 ACM SIGSAC conference on computer and communications security*. 67–82.

[59] Qin Wang, Ruijia Li, Qi Wang, and Shiping Chen. Non-fungible token (NFT): Overview, evaluation, opportunities and challenges 2021. *arXiv preprint arXiv:2105.07447*.

[60] Yishun Wang, Xiaoqi Li, Shipeng Ye, Lei Xie, and Ju Xing. Smart contracts in the real world: A statistical exploration of external data dependencies 2024. *arXiv preprint arXiv:2406.13253*.

[61] Martin White, Michele Tufano, Christopher Vendome, and Denys Poshyvanyk. Deep learning code fragments for code clone detection 2016. In *Proceedings of the 31st IEEE/ACM international conference on automated software engineering*. 87–98.

[62] Lei Xiao, Shuo Yang, Wen Chen, and Zibin Zheng. WakeMint: Detecting Sleep-minting Vulnerabilities in NFT Smart Contracts 2025. In *2025 IEEE International Conference on Software Analysis, Evolution and Reengineering (SANER)*. IEEE, 740–750.

[63] Xiaofei Xie, Tianlin Li, Jian Wang, Lei Ma, Qing Guo, Felix Juefei-Xu, and Yang Liu. Npc: Neuron path coverage via characterizing decision logic of deep neural

networks 2022. *ACM Transactions on Software Engineering and Methodology (TOSEM)* 31, 3, 1–27.

[64] Xiaofei Xie, Lei Ma, Felix Juefei-Xu, Minhui Xue, Hongxu Chen, Yang Liu, Jianjun Zhao, Bo Li, Jianxiong Yin, and Simon See. Deephunter: a coverage-guided fuzz testing framework for deep neural networks 2019. In *Proceedings of the 28th ACM SIGSOFT international symposium on software testing and analysis (ISSTA)*. 146–157.

[65] Shenao Yan, Guanhong Tao, Xuwei Liu, Juan Zhai, Shiqing Ma, Lei Xu, and Xiangyu Zhang. Correlations between deep neural network model coverage criteria and model quality 2020. In *Proceedings of the 28th ACM Joint Meeting on European Software Engineering Conference and Symposium on the Foundations of Software Engineering (FSE)*. 775–787.

[66] Shuo Yang, Jiachi Chen, Mingyuan Huang, Zibin Zheng, and Yuan Huang. Uncover the premeditated attacks: Detecting exploitable reentrancy vulnerabilities by identifying attacker contracts 2024. In *Proceedings of the IEEE/ACM 46th International Conference on Software Engineering*. 1–12.

[67] Yuanyuan Yuan, Qi Pang, and Shuai Wang. Revisiting neuron coverage for dnn testing: A layer-wise and distribution-aware criterion 2023. In *Proceedings of the IEEE/ACM 45th International Conference on Software Engineering (ICSE)*. 1200–1212.

[68] Jango Zhang. Combining GPT and Code-Based Similarity Checking for Effective Smart Contract Vulnerability Detection 2024. *arXiv preprint arXiv:2412.18225*.

[69] Lyuye Zhang, Kaixuan Li, Kairan Sun, Daoyuan Wu, Ye Liu, Haoye Tian, and Yang Liu. Acfix: Guiding llms with mined common rbac practices for context-aware repair of access control vulnerabilities in smart contracts 2024. *arXiv preprint arXiv:2403.06838*.

[70] Zhijie Zhong, Zibin Zheng, Hong-Ning Dai, Qing Xue, Junjia Chen, and Yuhong Nan. PrettySmart: Detecting Permission Re-delegation Vulnerability for Token Behaviors in Smart Contracts 2024. In *Proceedings of the IEEE/ACM 46th International Conference on Software Engineering*. 1–12.

[71] Di Zhu, Feng Yue, Jianmin Pang, Xin Zhou, Wenjin Han, and Fudong Liu. Bytecode similarity detection of smart contract across optimization options and compiler versions based on triplet network 2022. *Electronics* 11, 4, 597.

[72] Huanhuan Zou, Zongwei Li, and Xiaoqi Li. Malicious Code Detection in Smart Contracts via Opcode Vectorization 2025. *arXiv preprint arXiv:2504.12720*.